The Potential Therapeutic Effect of Cerebrolysin against Cyclosporine A-Induced Cerebellar Toxicity in Adult Male Albino Rats

Horeya Arafat[1], George Nagi Refaat[2], Mona M. Awny[3*], Ereny Fekry[1]

ABSTRACT

Cyclosporin A is an immunosuppressive agent used to treat organ rejection post-transplant and autoimmune diseases. It can induce toxic effects on the cerebellar cortex, such as cerebellar ataxia, vasogenic oedema, and occasional supratentorial lesions. Cerebrolysin possesses therapeutic strategies as a neurotrophic factor with neuroprotective effects. This work aims at evaluation of potential ameliorative Cerebrolysin effect on cerebellar toxicity induced by cyclosporine A in adult male albino rats. 40 adult male albino rats were randomized into 4 groups and received all treatments for 4 weeks. Group I served as control. In Group II, Cerebrolysin was given a daily intraperitoneal injection of 2.5 ml/kg. Group III received cyclosporin daily at a dosage of 25 mg/kg/day dissolved in olive oil, orally by gavage. Group IV, cyclosporin A concomitant with Cerebrolysin, was administered. After 4 weeks, animals were sacrificed by decapitation. Hematoxylin and Eosin staining was performed on the prepared sections, as was Cresyl fast violet, glial fibrillary acidic protein immunostaining, electron microscopic examination, and assessment of gait. Beside gait impairment, cyclosporin-treated animals showed irregular Purkinje and granule cells with irregular nuclei. Nerve fibers have a faint myelin sheath and/or focal areas of myelin splitting. Less abundant glial fibrillary acidic protein-positive cells and decreased Nissl's granules in perikarya. Cerebrolysin prevented most of the histopathological changes and locomotor behavior. Cerebrolysin has an ameliorative effect on cyclosporin A-induced cerebellar toxicity in adult male albino rats.

Introduction ·

An essential component of motor control is the cerebellum. It might also have a role in controlling emotional responses like fear and pleasure, as well as some cognitive processes like language and attention. Additionally, its most well-established

[1]*Histology and Cell Biology Department, Faculty of Medicine, Suez Canal University, Ismailia, Egypt.*
[2]*Internal Medicine & Cardiology Departments, Suez Canal Authority, Ismailia, Egypt.*
[3]*Forensic Medicine & Clinical Toxicology Department, Faculty of Medicine, Suez Canal University, Ismailia, Egypt.*
*Corresponding author
Mona Mohamed Awny
E-mail : mona_awny@med.suez.edu.eg
ORCHID : 0000-0002-1021-4163
Phone: 0097336121613

function is suggested to be related to movement. It has been reported that, although it does not start movement, the cerebellum helps with timing, coordination, and precision. It gathers information from the spinal cord sensory systems and from other regions of the brain, integrating it to adjust motor activity (Wright et al., 2016). Cerebellar damage has been suggested to cause problems with posture, motor learning, balance, and fine movement (El-azab et al., 2018). A fungus-derived molecule called cyclosporin-A (CsA) [Tolypocladium inflatum], discovered by Borel and Stahelin in 1970, hoping to develop a new antifungal treatment. Subsequently, its chemical structure and immunosuppressive properties were identified. Cyclosporin-A is a cyclic

endecapeptide that is lipophilic, neutral, and made up of 11 amino acids (Flores et al., 2019). It is an immunosuppressive medication used to prevent organ rejection after organ transplantation. According to reports, CsA is used to alleviate organ rejection after allogeneic heart, liver, and kidney transplants. It has also been suggested that it can be used in certain other autoimmune diseases, such as rheumatoid arthritis, when methotrexate has not sufficiently improved the illness. Additionally, CsA is a second-line medication used in bone marrow transplants to treat and prevent graft-versus-host disease. However, numerous adverse effects and toxicities were reported with CsA treatment, which include hypertension, arrhythmia, renal and hepatic toxicities, dyslipidemia, hypomagnesemia, hyperkalemia, gynecomastia, hypertrichosis, increased incidence of specific cancers, and neurotoxicity (Teimouri et al., 2022). Moreover, CsA treatment was reported to induce cerebellar ataxia in organ transplant patients (van Gaalen et al., 2014). Furthermore, toxic effects on cerebellar cortex were reported with CsA as reversible vasogenic oedema, frequently caused by posterior reversible encephalopathy syndrome, as well as occasional supratentorial lesions (Roshan et al., 2017). Cerebrolysin is a low-molecular-weight neuropeptide that possesses neurodegenerative capabilities and is produced using particular manufacturing and laboratory procedures from an extract of pig brain tissue. Cerebrolysin has been shown to have various positive benefits in both in vitro and in vivo research, including a reduction in excitotoxicity, free radical production, neuroinflammation and/or activation of microglia and calpain activation or apoptosis (Masliah and Díez-Tejedor, 2012). Induction of neural sprouting in tissue culture, neurotropic effects, and improving neural survival in ischemic situations are some of cerebrolysin's further remarkable actions on neural tissue (Zhang et al., 2013; Ruozi et al., 2015). Moreover, cerebrolysin was reported to reduce central and peripheral neuropathy as a result of chronic hyperglycemia induced by streptozotocin in mice and rats (Zurita et al., 2017). It has also been suggested that cerebrolysin could protect against spinal cord pathology and hyperalgesia that induced nerve lesions (Sharma et al., 2023).

Limited histological studies demonstrated either the toxic effect of cyclosporine or the beneficial effects of cerebrolysin on the cerebellar cortex (Sherif, 2017). Moreover, no available histological studies investigated the potential ameliorative effect of cerebrolysin against cyclosporine A induced cerebellar toxicity. In order to investigate such a role, the current work was established using light; either histological or immunohistochemical techniques; and electron microscopic examinations beside footprint analysis.

Material and Methods

This research was conducted in the Faculty of Medicine, Suez Canal University, Ismailia, Department of Histology and Cell Biology. Animal care was carried out in accordance with its institutional policies (Code number: 5284).

Experimental animals

Forty mature male albino rats of the same age (3 months) and weight (150–180 g) were used in the experiment. Animals were purchased from the Suez Canal University Faculty of Medicine's Centre of Excellence for Animal Care. Prior to the trial, rats were housed for two weeks to allow for acclimatization. They were given a standard, balanced feed and free access to water while

living in stainless steel cages at room temperature in a well-ventilated animal house.

Drug preparation

- Cyclosporin was purchased from Novartis Pharma Company with a commercial name (Sandimmun Neoral) in the form of soft gelatin capsules, each containing 50 mg cyclosporine A.
- Olive oil, from the commercial market.
- Ebewe Pharmaceuticals manufactured ampoules containing 1 or 5 millilitres of cerebrolysin that were used in this study.
- Glial Fibrillary Acid Protein (GFAP) was obtained from Thermo Scientific Company.

N.B. All drugs were prepared immediately before administration.

Experimental design

Rats were randomly subdivided by using a random number table into 4 groups (10 animals each). All treatments were given for 4 weeks.

- *Group I* (the control group) consists of 10 rats and was subdivided into two equal subgroups of five rats each:
  - Group Ia: negative control group, in which the animals were not given any therapy.
  - Group Ib: positive control group that was administered olive oil daily by gavage at a dose of 0.5 ml for 4 weeks (Abdelkader et al., 2021).
- *Group II* (Cerebrolysin Group): animals in this group were given a daily 2.5 ml per kilogramme intraperitoneal injection (I.P.) of cerebrolysin for 4 weeks (Makary et al., 2015).
- *Group III* (Cyclosporin A group received cyclosporine daily at a dose of 25 mg/kg per day, dissolved in olive oil, orally by gavage for 4 weeks (Abdelkader et al.,

2021). This dose is double the therapeutic dose (Feagan et al., 1994) and approximately 1/59 of LD50. After oral administration, the LD50 of cyclosporine is 1480 mg/kg (Sovcikova et al., 2002).

- *Group IV* (Cyclosporin A + Cerebrolysin): cyclosporine A was administered concomitantly with cerebrolysin with the same previous doses and duration.

Footprint analysis

Gait assessment was performed by foot-print analysis on the four experimental rat groups using an 80-cm footprint paper sheet within a preformed walking platform. Each rat was trained for three days before evaluation so that it would cross the platform without hesitating. Food rewards were used as positive motivators during training days. Rats were then subjected to gait assessment at the end of the experiment. The gait test was analyzed by having the animal walk across an ink pad and then a paper sheet so that the spatial pattern of the ink prints could be measured. For each rat, the data from three successive runs were averaged. On footprints, stride length and stride width were measured. Stride length represented the separation in distance between the successive contacts of the same paw, whereas stride width represented the distance made by two successive contralateral hind-steps made at 90° to the direction of travel (Kara et al., 2021; Mahmoudi et al., 2022; DeAngelo et al., 2023).

Tissue sample collection

All animals were sacrificed by decapitation under light anaesthesia after 4 weeks of injections of different treatments. Then samples were collected.

Light microscopic study

The animals' resected cerebella were quickly excised, chopped into small pieces, and fixed in formalin (10%) for 48 hours. They were subsequently dried in increasing amounts of alcohol, cleared in xylene, and ultimately embedded in paraffin. Staining of the serial coronal slices, each measuring about 5μm thick, with the following stains (Layton and Suvarna, 2013):

1. **Haematoxyline and Eosin (H&E):** to determine the cerebellum's general architecture.
2. **Cresyl fast violet**: for demonstration of Nissl granules.

Immunohistochemical study

The following steps were taken into consideration for the immunohistochemical study: fixation in 10% formalin for 2 days, dehydration, clearing, and ultimately becoming paraffinized. Five μm-thick paraffin slices were cut. For the purpose of displaying the astrocytes, staining of sections was done using a modified avidin-biotin peroxidase approach for glial fibrillary acidic protein (GFAP). All portions were moistened and deparaffinized. To reveal the antigen, sections were exposed to 0.01 M citrate buffer with pH 6.0 for approximately 10 minutes. Then the endogenous peroxidase activity effect was eliminated by incubating the sections in 0.3% H_2O_2 for 12 hours before blocking with 5% horse serum for 1-2 hours. The slides were first washed and incubated at 4 $C^°$ for 18–20 hours with the primary antibody (1:100 monoclonal mouse anti-GFAP). The sections were then mounted, dehydrated, and stained with hematoxylin on slides prepared with 0.05% diaminobenzidine. The GFAP+ve cells were brownish in color with blue-colored nuclei (Cattoretti et al., 1993). The exact same procedure was followed while processing negative controls, with the exception of using the primary antibody. A brain slide was used as a positive control (Mohamed and Mohamed, 2018). Each image has a resolution of 10 MP (megapixels) (3656 x 2740 pixels) and was taken by a calibrated digital standard microscope camera (Tucsen ISH1000 digital microscope camera) and an Olympus CX21 microscope. For image capture and enhancement, "IS Capture" software was used.

Morphometric study:

Using software Image J. for measuring the area percent of Nissl's granules in cresyl violet-stained sections. The area percent for GFAP cytoplasmic immunoreaction in the bodies of astrocytes and their processes in cerebellar cortices was also measured.

Electron microscopic study:

Each group's cerebella were dissected for electron microscopic examination. After 24-48 hours of dissection, specimens (1x1 mm) were promptly cut and preserved in 4% cold glutaraldehyde. Then post-fixation was done in 1% OsO4 for two hours, rinsed four times in the same buffer (phosphate buffer, pH 7.2), and dried. Ascending degrees of alcohol (30, 50, 70, 90, and 100% for 2 hours) were used to dehydrate the subject before embedding it in an epon araldite mixture. Toluidine blue was used to stain 0.5μm-thick semithin slices. The selected areas were divided into ultrathin pieces of 50 nm thickness, which were stained with uranyl acetate and lead citrate (Hayat, 2000). With a transmission electron microscope (Joel JEM-100 CXII; Joel, Tokyo, Japan), the ultrathin sections were imaged in the electron microscopic unit, Faculty of Science, Ain Shams University, Egypt.

Statistical analysis:

For data entry, Microsoft Excel from the Microsoft Office 365 Software Package (from Microsoft Corporation, USA) was used. The mean and standard deviation (SD) of the data were entered. Then the results were analyzed using one-way analysis of variance (ANOVA) and the post-hoc Tukey test to look for variations in histopathological abnormalities between groups. To evaluate statistical significance, a P-value of under 0.05 was applied.

Results

Footprint analysis

On the footprint sheets, the rat gait patterns from the various groups are depicted (Figure 1A). At the conclusion of the experiment, stride length did not significantly vary in any of the experimental groups (Figure 1B). Cyclosporin-treated rats showed significantly reduced stride width compared to the other groups, whereas co-treatment with Cerebrolysin significantly increased the stride width (Figure 1C).
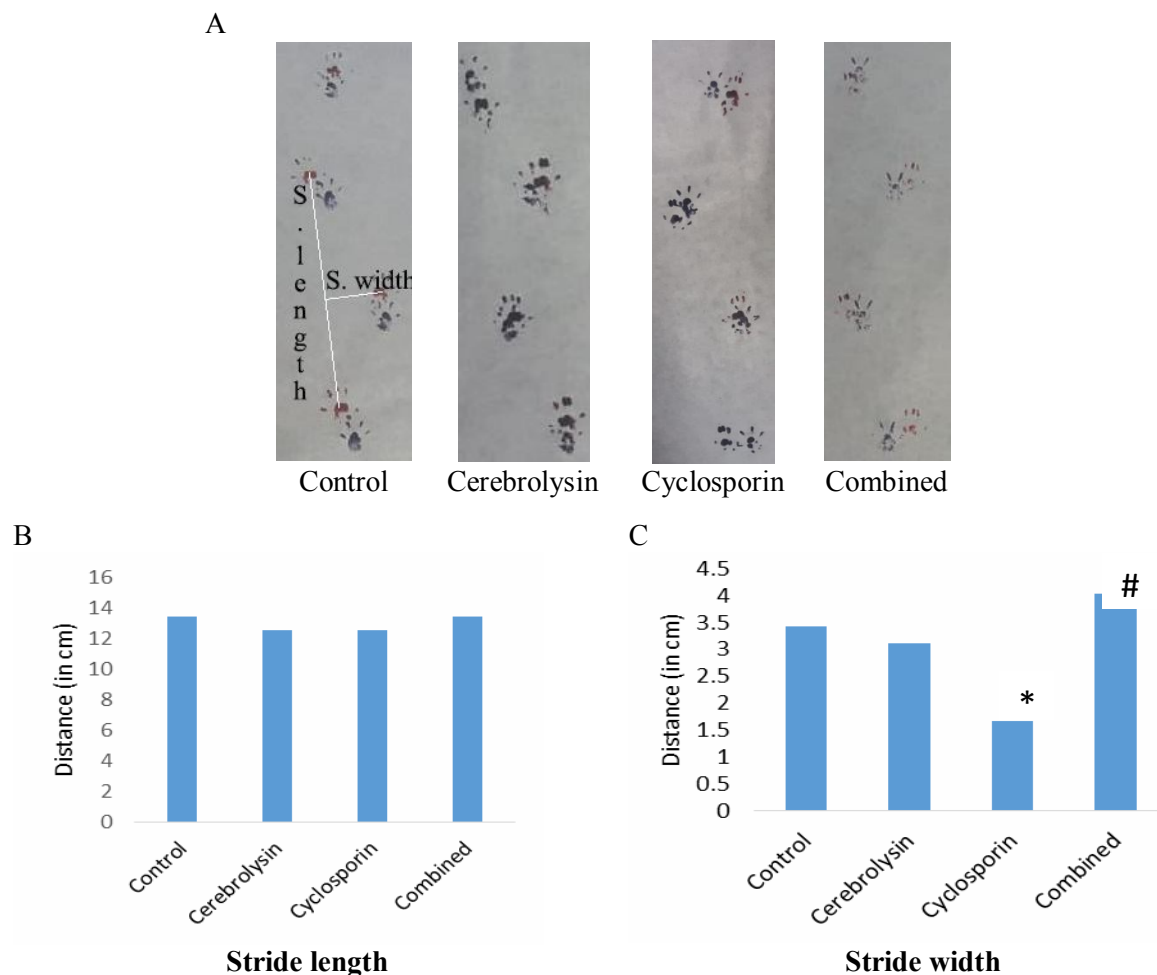

Fig. (1): A: The gait patterns of the rats in the experimental groups B: Stride length in all the experimental groups shows no significant changes. C: Stride width is significantly reduced in the cyclosporin A group (*) in comparison to the control group. The combined group (Cyclosporin A + Cerebrolysin) shows significant improvement in stride width (#) compared to the cyclosporin A group.

Light microscopic findings

Group Ia (the -ve control group) demonstrated normal white matter and cerebellar cortex architecture when the cerebellum was stained with H&E. In the molecular layer, the cortex is depicted as a scattering of minute stellate and basket cells. The Purkinje cell layer displayed large pyriform cells with vesicular nuclei and apical dendrites. In the granular layer, crowded tiny granule cells with intensely marked nuclei were also visible (Figure2A). Group Ib (+ve control group) was nearly similar to the negative one. Group II (cerebrolysin) is almost as the control (Figure2B). Group III (cyclosporin A) showed widely displaced, distorted and shrunken Purkinje cell, leaving wide intercellular spaces. Complete absence of Purkinje cells was also shown (Figure2C). Group IV (cyclosporin A + cerebrolysin) Purkinje cells were almost as to that of the control group. However, few distorted and shrunken Purkinje cells and wide intercellular spaces were still show (Figure2D).
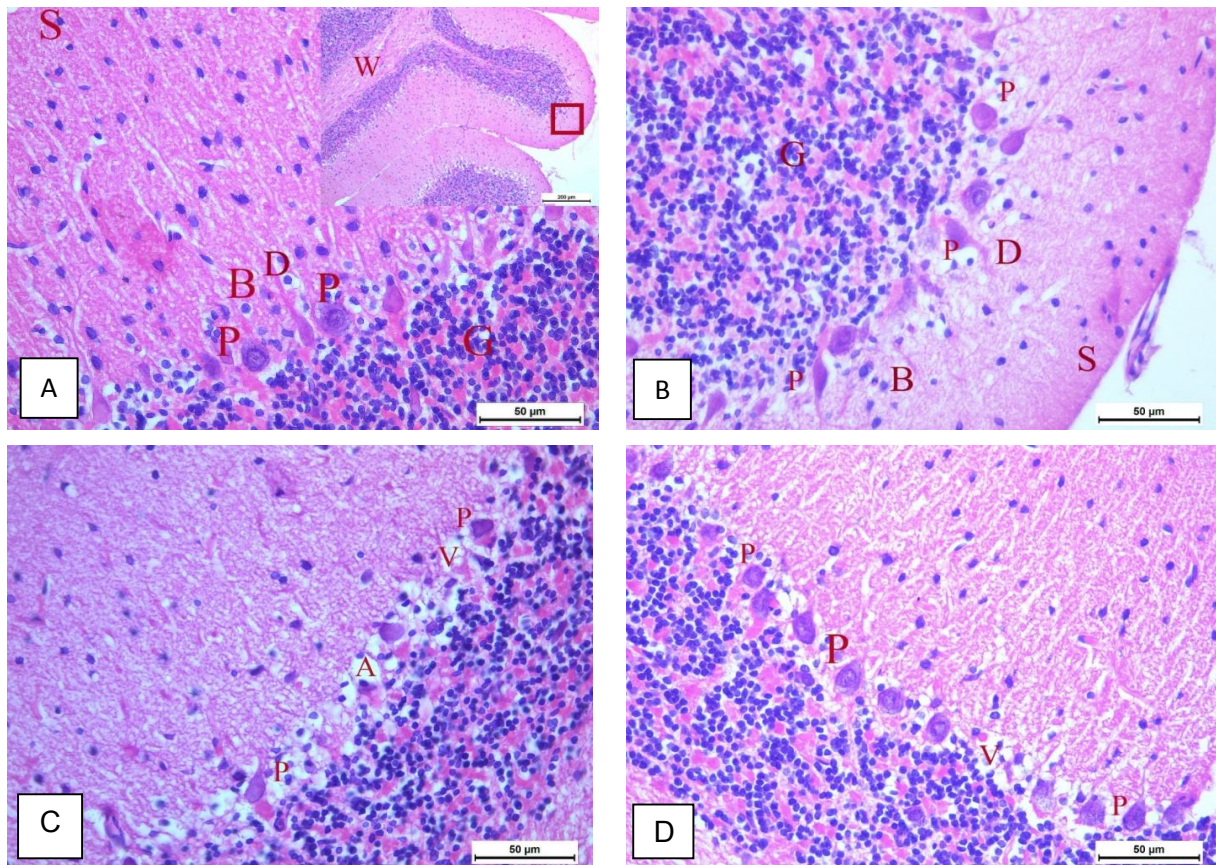

Fig. (2): Photomicrographs showing a section of a rat's cerebellum stained with H&E X 400 from different groups. A. **(Negative control group)** inset x100 shows normal architecture of cerebellar cortex and white matter (W). In the molecular layer, the cortex shows dispersed tiny stellate (S) and basket cells (B). In the Purkinje cell layer, large pyriform cells with vesicular nuclei (P) and apical dendrites (D) are shown. In the granular layer, there are a lot of small granule cells with deeply pigmented nuclei (G). **B. (Cerebrolysin group)** is almost similar to control group. **C. (Cyclosporin A group)** shows widely displaced, distorted and shrunken Purkinje cell (P), leaving wide intercellular spaces (V). Complete absence of Purkinje cells (A) is also shown. **D. (Cyclosporin A + Cerebrolysin)** group shows Purkinje cells (P) almost similar to control group. However, few distorted and shrunken Purkinje cells and wide intercellular spaces (V) are still shown.

Cresyl fast violet stained sections in the both the cerebrolysin and negative control groups' cerebellar cortex (Groups Ia& II),in the perikarya purple Nissl's granules of large pyriform Purkinje cells (Figure 3A & Figure 3B). Group Ib (positive control group) was nearly as to the negative one. Group III (cyclosporin A) showed decreased purple Nissl's granules in the perikarya of Purkinje cells, which was statistically significant compared to the control group (Figure3C &Figure4). Group IV (cyclosporin A + cerebrolysin) showed Purkinje cell perikarya had more purple Nissl's granules; which was statistically significant compared to cyclosporin A -treated rats (Figure 3D & Figure 4).
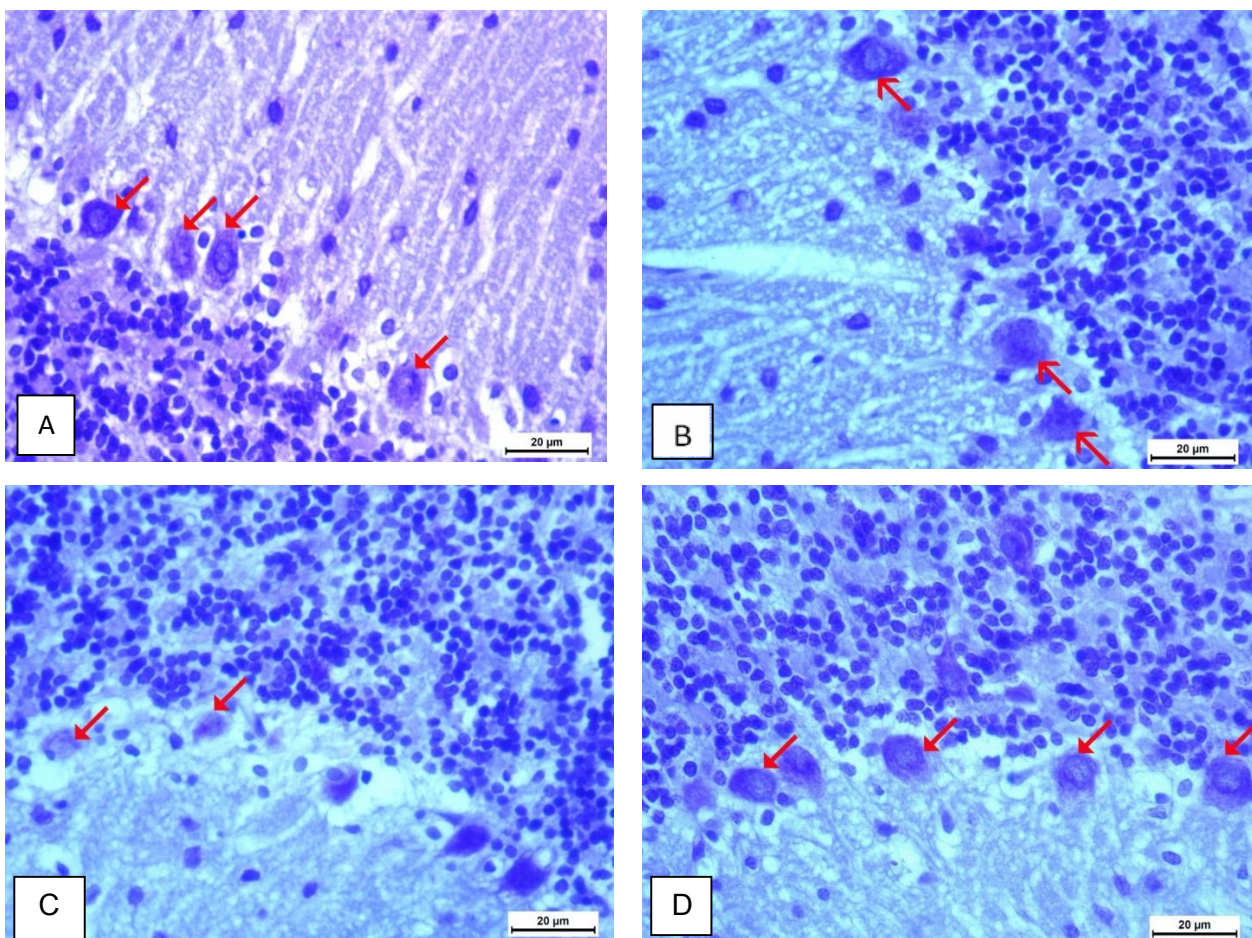

Fig. (3): Photomicrographs of a section in the cerebellar cortex stained with cresyl fast x 630 from different groups. **A&B.** Both **(Negative control group)** and **(Cerebrolysin group)** show purple Nissl's granules can be seen in the perikarya of large pyriform Purkinje cells (arrows). **C. (Cyclosporin A group)** shows less purple Nissl's granules (arrows) in the perikarya of Purkinje cells. **D. (Cyclosporin A + Cerebrolysin)** group shows incresed purple Nissl's granules (arrows) in the perikarya of Purkinje cell compared to that of the Cyclosporin A group.
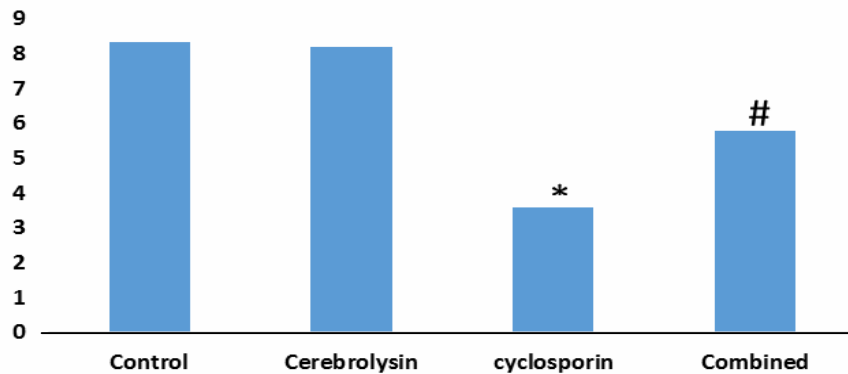
Fig. (4): The mean area percent of Nissl's granules in the different studied groups.
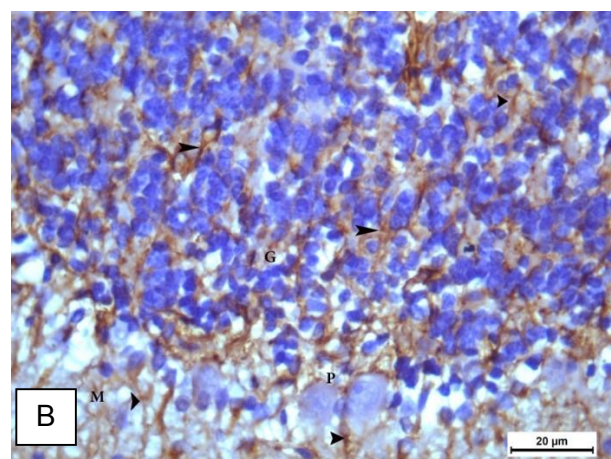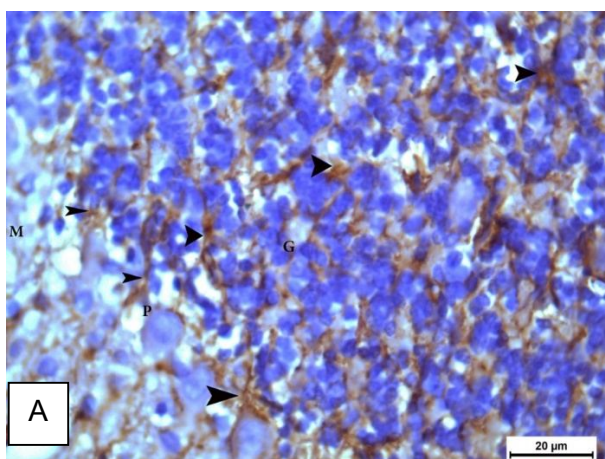*Statistically significant compared to the control group (P<0.01),
Statistically significant compared to the cyclosporin A group (P<0.01)

Immunohistochemical findings

Rat cerebellar cortex sections stained with glial fibrillary acidic protein (GFAP) revealed dispersed GFAP positive immunoreactive cells with thin long processes in Group Ia (negative control group) [cytoplasmic reaction] in the molecular, Purkinje, and granular cortical layers (Figure5A).Group Ib (positive control group) was nearly as to the negative one. Group II (cerebrolysin group) showed immunoreactive cells nearly similar to control group (Figure5B). Group III (cyclosporin A group) showed different cortical layers had less often appearing GFAP positive cells, which was statistically significant when compared to the control group. (Figure 5C & Figure 6). Group IV (cyclosporin A + cerebrolysin) revealed GFAP expression that was positive, more or less in line with what was observed in the control rats, and this was statistically significant compared to cyclosporin A - treated rats (Figure 5D & Figure 6).
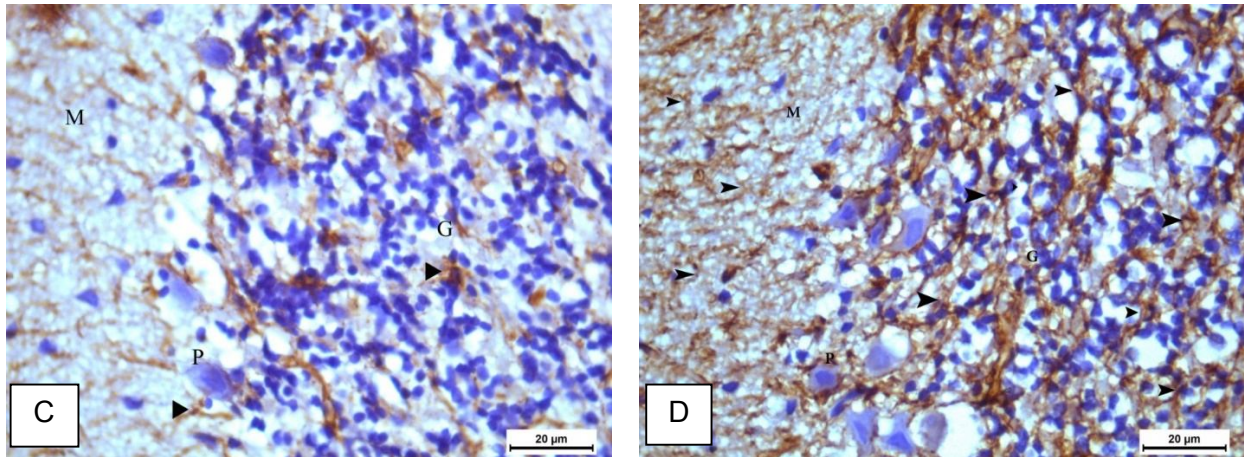
Fig. (5): Photomicrographs of GFAP immunohistochemically stained sections of rat cerebellar cortex x 630. **A. (Negative control group)** shows scattered positive GFAP immunoreactive cells with long and thin processes (arrow heads) in the different cortical layers; molecular (M), Purkinje (P) and granular (G); **B. (Cerebrolysin group)** shows positive GFAP immunoreactive cells almost as control group. **C. (Cyclosporin A group)** shows less abundant GFAP positive cells in different cortical layers (arrow heads) as compared with that of the control; **D. (Cyclosporin A + Cerebrolysin) group** shows increased expression of GFAP positive cells which is more or less similar to that noticed in the control rats (arrow heads).
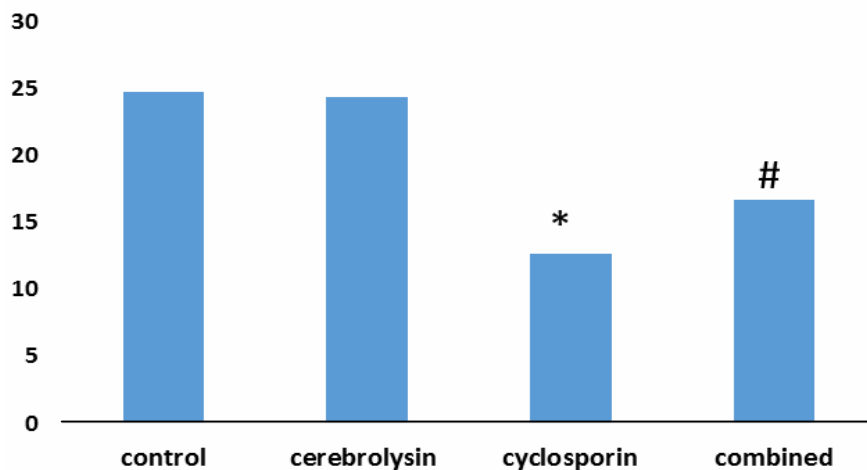

Fig. (6): The mean area percent of astrocytic GFAP activity in the different study groups.
*Statistically significant compared to the control group (P<0.01),
Statistically significant compared to the cyclosporin A group (P<0.0)

Electron microscopic findings

Group Ia (negative control group) showed Purkinje cells with its main dendrite. The nuclear envelope's indentation and the large oval euchromatic nucleus with a clearly defined nucleolus were visible. Rough endoplasmic reticulum cisternae (RER) were well-developed and visible in the cytoplasm (Figure7A). Group Ib (positive control group) was nearly as to the negative one. Group II (cerebrolysin group) showed Purkiinje cell nearly similar to control group with large euchromatic nucleus with and well- defined nucleolus. Granule cells and nerve fibers were also shown (Figure7B).Group III (cyclosporin A group) showed two Purkinje cells both with irregular nuclei which was markedly shrunken and without nucleoli in one of them. Irregular granule cells, nerve fiber with faint myelin sheath and empty spaces between the cells in the neuropil were also shown (Figure7C). Group IV (cyclosporin A + cerebrolysin) showed Purkinje cells with its main dendrite and large oval euchromatic nucleus nearly similar to that of the control group. Slightly irregular nucleus of another Purkinje cells and the few empty areas in the neuropil were also shown (Figure7D).

Group Ia (negative control group) showed Purkinje cells with large oval euchromatic nucleus. Numerous mitochondria and numerous, well-developed RER cisternae were visible in the cytoplasm (Figure 8A).Group Ib (positive control group) was almost similar to the negative one. Group II (cerebrolysin group) showed Purkiinje cell nearly as to control group with large oval euchromatic nucleus and well- defined nucleolus. The cytoplasm also displayed well-developed RER cisternae, free ribosomes, lysosomes, and mitochondria (Figure8B). Group III (cyclosporin A group) showed Purkiinje cell with irregular and markedly shrunken nuclei without nucleoli. The cytoplasm showed few scattered rough endoplasmic reticulum tubules and lysosomes. Notably, there were no mitochondria in the cytoplasm. The neuropil also displayed vacuolations in the cytoplasm and empty spaces between the cells (Figure8C).Group IV (cyclosporin A + cerebrolysin) showed large oval euchromatic nucleus in Purkinje cells. Numerous mitochondria, well-developed rough endoplasmic reticulum cisternae, and lysosomes were visible in cytoplasm (Figure8D).
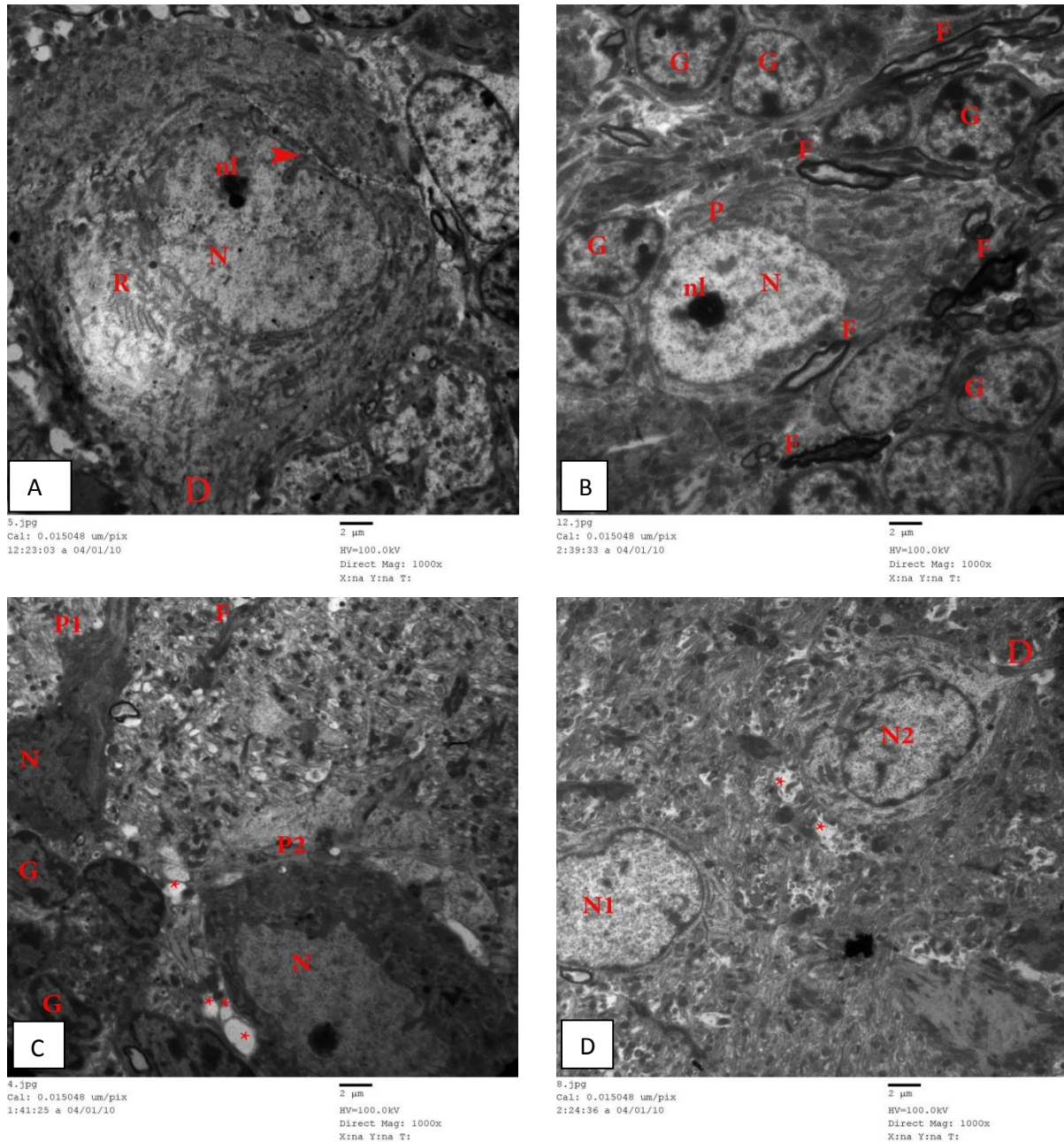
Fig. (7): Transmission electron microscope photomicrographs showing Purkinje cells of rats' cerebellum x 1000. **A. (Negative control group)** shows Purkinje cells with its main dendrite (D). Large oval euchromatic nucleus (N) with indentation of the nuclear envelope (arrow head) and well-defined nucleolus (nl) are shown. The cytoplasm shows well-developed rough endoplasmic reticulum cisternae (R). **B. (Cerebrolysin group)** shows Purkiinje cell (P) nearly almost as control group with a large euchromatic nucleus (N) and a well- defined nucleolus (nl). Granule cells (G) and nerve fibers (F) are also shown. **C. (Cyclosporin A group)** shows Purkinje cells (P1 & P2) both with irregular nuclei (N) which is markedly shrunken and without nucleoli in P1. Irregular granule cells (G), nerve fiber with faint myelin sheath and empty areas in the neuropil (*) are also shown. **D. (Cyclosporin A + Cerebrolysin) group** shows Purkinje cells with its main dendrite (D) and large oval euchromatic nucleus (N1) nearly similar to that of the control group. Slightly irregular nucleus (N2) of another Purkinje cell and few empty spaces in the neuropil (*) are also shown.
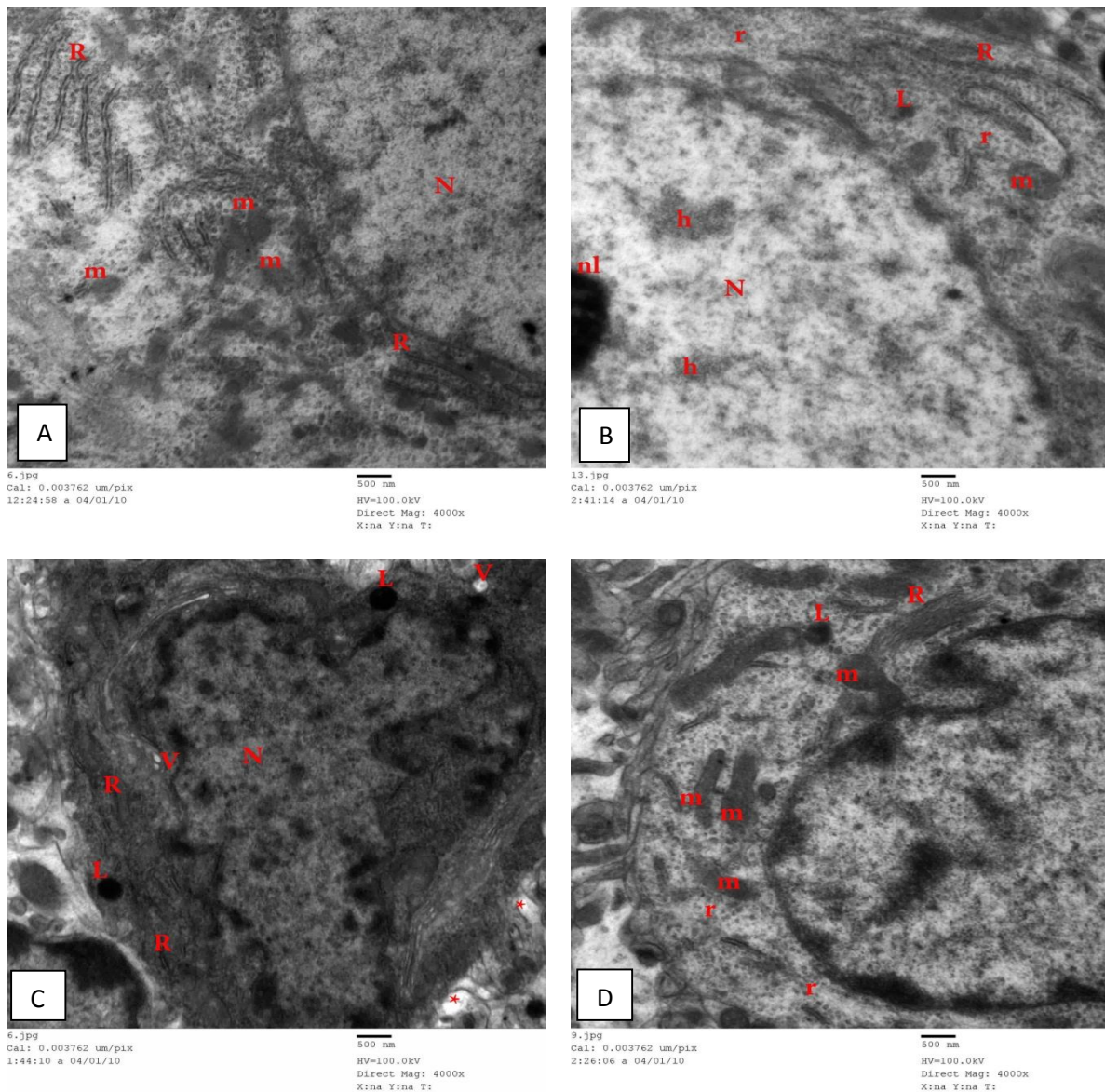
Fig. (8): Photomicrographs of transmission electron microscope demonstrating Purkinje cell of cerebella of different groups x 4000. **A. (Negative control group)** shows Purkinje cells with a large oval euchromatic nucleus (N). Numerous mitochondria (m) and many well-developed rough endoplasmic reticulum cisternae (R) are shown in the cytoplasm. **B. (Cerebrolysin group)** shows Purkiinje cell nearly similar to that of the control group, with its large oval euchromatic nucleus (N)   well- defined nucleolus (nl) and heterochromatin islands (h). Well-developed rough endoplasmic reticulum cisternae (R), free ribosomes (r), lysosome (L) and mitochondria (m) are also shown in the cytoplasm. **C. (Cyclosporin A group)** shows Purkiinje cell with irregular and markedly shrunken nuclei (N) without nucleoli. The cytoplasm shows few scattered rough endoplasmic reticulum cisternae (R) and lysosomes (L). Notice no mitochondria are shown in the cytoplasm. Vacuolations in the cytoplasm (V) and empty spaces in the neuropil (*) are also shown. **D. (Cyclosporin A + Cerebrolysin) group** shows Purkinje cells with large oval euchromatic nucleus (N). The cytoplasm shows numerous mitochondria (m), well-developed rough endoplasmic reticulum cisternae (R) and lysosomes (L).

Multiple granule cells with rounded or oval nuclei and clusters of heterochromatins were visible in Group Ia (the negative control group). Multiple nerve fibers with dark myelin sheath were shown. Astrocytes with electron dense cytoplasm were also shown (Figure9A). Group Ib (positive control group) was nearly as to the negative one. Group II (cerebrolysin group) was almost similar to the control group, which also included many granule cells with rounded or oval nuclei with its heterochromatin. Some myelinated nerve fibers were also shown (Figure9B). Group III (cyclosporin A group) showed multiple granule cells with irregular nuclei. The neuropil has empty areas and some nerve fibers (Figure 9C). Group IV (cyclosporin A + cerebrolysin) showed granule cells almost like the control group with heterochromatin aggregates in their spherical or oval nuclei. Astrocyte with electron dense cytoplasm and well-myelinated nerve fibers were also shown. However, vacuolations in axoplasm of few nerve fibers and the spaces in the neuropil were also shown (Figure9D).

Group Ia (negative control group) revealed granule cells with nucleus that was rounded or oval with cluster of heterochromatin and well-defined nucleolus. Numerous mitochondria and some lysosomes were shown in the surrounding cytoplasm (Figure 10A). Group Ib (positive control group) was nearly similar to the negative one. Group II (cerebrolysin group) was nearly similar as to control group exhibited heterochromatin-clumped granule cell nucleus which was oval to round. Some mitochondria, lysosomes and free ribosomes, in the surrounding cytoplasm, were also shown (Figure10B). Group III (cyclosporin A group) showed granule cells with irregular nuclei. In the neuropil, empty space and certain nerve fibres with isolated areas of myelin sheath splitting were also visible (Figure10C). Group IV (cyclosporin A + cerebrolysin) showed granule cell almost the same to control group with oval or rounded nucleus (N) with heterochromatin clumps. The surrounding rim of cytoplasm contained free ribosomes and mitochondria (Figure10D).
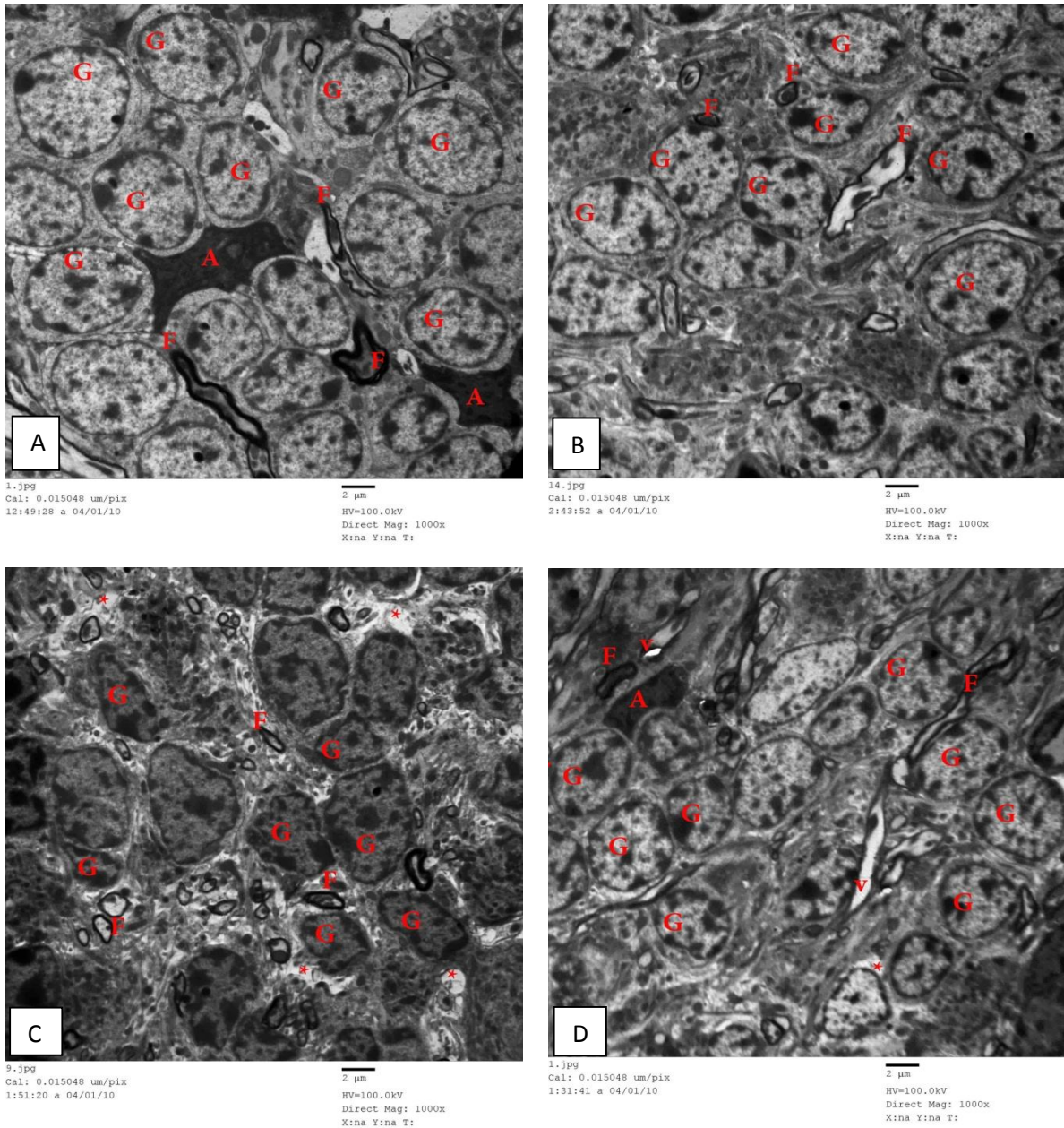
Fig. (9): TEM photomicrographs of the granule cells of cerebellum of rats in different experimental groups x 1000. **A. (Negative control group)** shows numerous granule cells (G) with rounded or oval nuclei with heterochromatin clumps**.** Multiple nerve fibers (F) with dark myelin sheath are shown. Astrocytes (A) with electron dense cytoplasm are also shown. **B. (Cerebrolysin group)** shows multiple Granule cells (G) nearly similar to that of the control groups, having rounded or oval nuclei and with clumps of heterochromatin. Some myelinated nerve fibers (F) are also shown. **C. (Cyclosporin A group)** shows multiple granule cells (G) with irregular nuclei. Some nerve fibers (F) and empty spaces in the neuropil (*) and are also shown. **D. (Cyclosporin A + Cerebrolysin) group** shows granule cells (G) nearly similar to control group, with rounded or oval nuclei with clumps of heterochromatin. Astrocyte (A) with electron dense cytoplasm and well-myelinated nerve fibers (F) are also shown. However, vacuolations (v) in the axoplasm of few nerve fibers and empty spaces in the neuropil (*) are also shown.
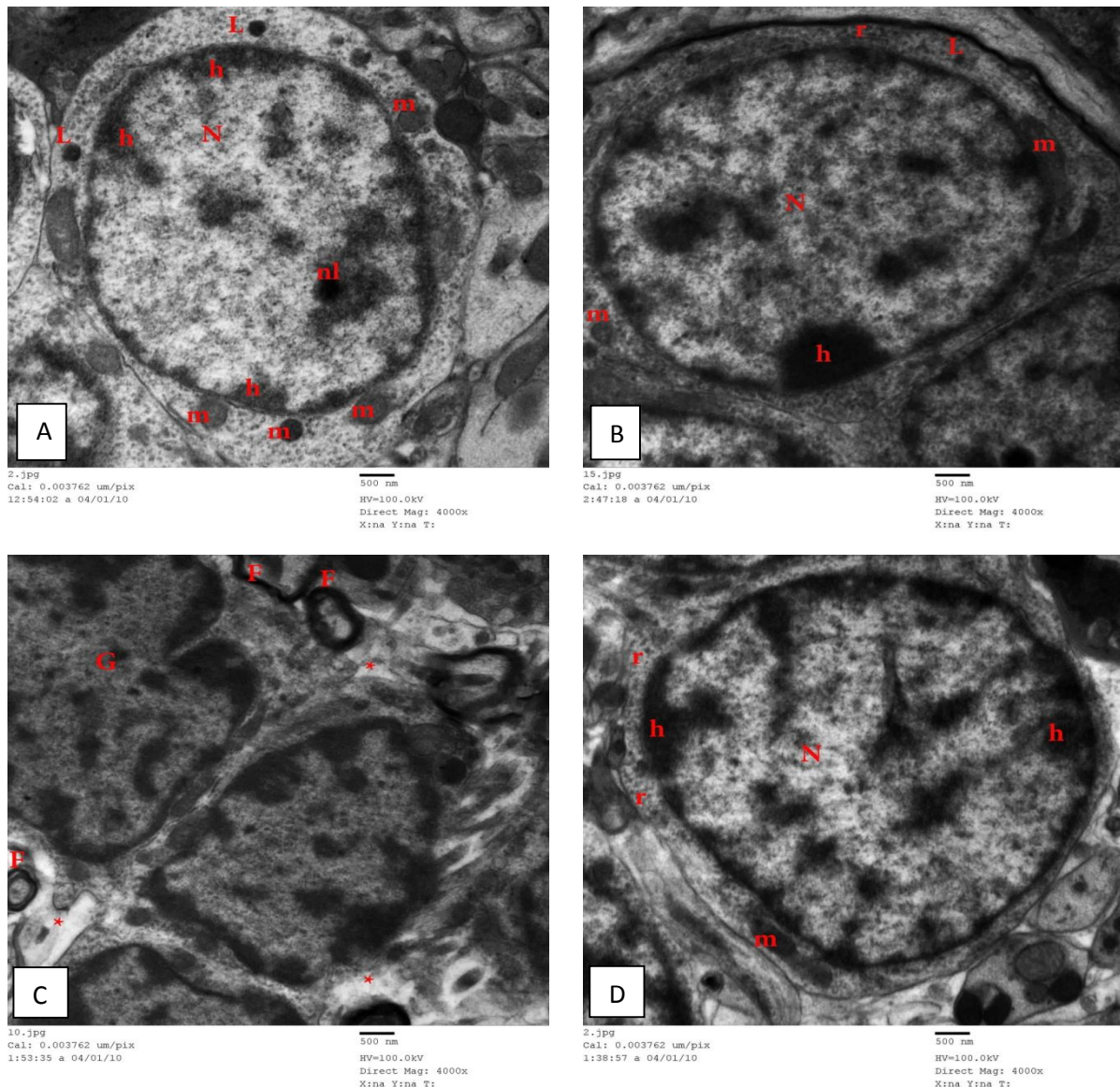
Fig. (10): TEM photomicrographs of granule cells (G) in the cerebellum of rats x 4000. **A. (Negative control group)** shows granule cell with rounded or oval nucleus (N) and heterochromatin clumps (h) and well-defined nucleolus (nl). Granule cell nucleus is surrounded by a rim of cytoplasm that shows numerous mitochondria (m) and some Lysosomes (L). **B. (Cerebrolysin group)** shows granule cell nearly similar to control group with rounded or oval nucleus (N) and clumps of heterochromatin (h).Some mitochondria (m), lysosomes (L) and free ribosomes (r), in the surrounding cytoplasm, are also shown. **C. (Cyclosporin A group)** shows granule cells (G) with irregular nuclei. Empty spaces in the neuropil (*) and some nerve fibers (F) with focal areas of splitting of their myelin sheath are also shown. **D. (Cyclosporin A + Cerebrolysin) group** shows granule cell nearly similar to control group with rounded or oval nucleus (N) and heterochromatin clumps (h). Mitochondria (m) and free ribosomes (r) are shown in the rim of cytoplasm that surrounds the nucleus (N).

Discussion

Cyclosporine is an immuno-suppressive medication that is used to treat post-transplant organ rejection. Additionally, it is used to treat post-transplant rejection following allogeneic kidney, liver, and heart transplants, as well as rheumatoid arthritis, when methotrexate has not sufficiently alleviated symptoms. It is also a second-line treatment in the treatment regimen for graft vs. host disease and ALS. Additionally, it was mentioned that Behcet disease and refractory posterior uveitis are both indicated uses for cyclosporin (Pharmacoeconomic Review Report, 2018; Ponticelli and Glassock, 2019; Pradier et al., 2019; Sun et al., 2019; Xin et al., 2019). Cyclosporine-induced cerebellar toxicity was reported in the form of cerebellar ataxia in organ transplant patients (van Gaalen et al., 2014). Additionally, transient supratentorial lesions and reversible vasogenic oedema of the cerebellum and white matter [usually from posterior reversible encephalopathy syndrome] were also reported (Roshan et al., 2017).

The control and cerebrolysin groups in the current study showed normal histological structures of the cerebellum that were in accordance with what was described by Mescher (2016) and Ovalle and Nahirney (2000).

In the current study, in the cyclosporine A-treated group (group III), animals were given a daily dose of 25 mg/kg of CsA dissolved in olive oil orally by gavage for 4 weeks (Abdelkader et al., 2021). This dose is double the therapeutic dosage (Feagan et al., 1994).

The present study showed that examined H and E-stained sections of cyclosporine A-treated groups (group III), revealed widely displaced, distorted, and shrunken Purkinje cells, leaving wide intercellular spaces. A complete absence of Purkinje cells was also noticed. The results of the TEM examination of cyclosporine-treated animals confirmed those of the light microscope. Purkinje cells were found to have markedly shrunken and irregular nuclei without nucleoli. The cytoplasm showed few lysosomes and dispersed rough endoplasmic reticulum tubules. In the cytoplasm, there were no mitochondria to be found. The neuropil also displayed empty spaces. Additionally, irregular granule cells with irregular nuclei were also shown. Nerve fibers with a weak myelin sheath and/or focal areas of myelin sheath splitting were also shown. Limited available histological studies demonstrated cyclosporine A's adverse effects on the cerebellar cortex using a light microscope. Additionally, no previous studies investigated such effects using an electron microscope. Abdelkader et al. (2021) attributed cyclosporine A's toxic effects to oxidative stress. They observed that the harmful effects of cyclosporine A on kidney morphology and function were brought on by oxidative stress and enhanced reactive oxygen species (ROS) production. This was in agreement with our results related to the absence of mitochondria in the cytoplasm of the Purkinje cells.

Some studies believed that the Purkinje and granular cells were the direct targets for any poisonous chemical in the cerebellum, which is consistent with our findings about degenerative alterations in Purkinje and granular cells (Fonnum and Lock, 2000). Lu et al. (2020) investigated CsA-induced nephrotoxicity by increasing reactive oxygen species (ROS) and malonaldehyde (MDA) levels and reducing glutathione (GSH) and superoxide dismutase (SOD) levels. These morphological changes resulted in vascular abnormalities, atrophy of the tubules, fibrosis of the interstitium,

apoptosis of the tubules, and ultimately renal dysfunction. Apoptosis can explain the presence of cytoplasmic vacuolation in our results. Other researchers investigated cyclosporin A hepatotoxicity and attributed it to the oxidative stress caused by cyclosporin A (Khalaf et al., 2017; Vangaveti et al., 2021; Faheem et al., 2022).

Rafati et al. (2015) reported that disturbance of the astrocyte's architecture caused cerebellar Purkinje cells to degenerate. Thus, cyclosporine-induced loss of the supporting astrocyte in the cerebellum results in degeneration of Purkinje cells in such a group.

Additionally, Purkinje cells shrank and withdrew their protoplasmic processes as a result of the breakdown of their cytoskeletal components (Shalabi and Sarhan, 2008). This can explain the presence of empty areas in the neuropil. Weil et al. (2016) attributed demyelination to a degenerating nerve's increased water content, which results in intramyelinic swelling and edematous splitting at different levels of the myelin lamella. Immunohistochemical examination of sections stained with glial fibrillary acidic protein (GFAP) of the cyclosporin group revealed fewer available GFAP+ve cells that were shown in different layers as compared to the control group. (GFAP) is an intermediate filament-III protein that is only present in enteric glial cells, non-myelinating Schwann cells, and astrocytes in the CNS (Yang and Wang, 2015).

It was reported that microglia, which are considered the primary immune cells of the CNS, play an important role in the control of the innate immune response, although astrocytes also play a role. Astrocytes were also reported to be one of the earliest cell types to get a CNS viral infection. Additionally, astrocytes express multiple receptors known as pattern recognition receptors (PRRs) that can identify viral particles and set off signaling cascades that cause astrocytes to release inflammatory cytokines, which then prompt an innate immune response and include astrocytes in CNS immunological functions. Accordingly, less abundant GFAP-positive cells in the cyclosporine group can be attributed to damage to astrocytes by the immunosuppressive effect of cyclosporin A (Liddicoat and Lavelle, 2019; Jorgaevski and Potokar, 2023).

Cresyl-fast violet-stained sections in the cerebellar cortex showed the perikaryal of group III Purkinje cells that have fewer purple Nissl granules. Reduced Nissl's granules, known as chromatolysis, were found to be mostly triggered by apoptosis in Wistar rat neurons (Nagib et al., 2018).

From the cerebellar cortex to the brainstem, Purkinje cells project a significant quantity of GABAergic input, which controls the output of these nuclei in motor function (Hasan et al., 2020). In the current research, cyclosporine medication reduced stride width, which demonstrated that cyclosporine impaired motor coordination.

Despite cyclosporin A's toxicity, due to its effectiveness as a treatment, it continues to be one of the most frequently used immunosuppressive drugs (Faheem et al., 2022). Moreover, Shah et al. (2017) reported that CsA was still the basis of organ transplants in spite of its adverse effects. Thus, it is crucial to search for ameliorative agents to ameliorate cyclosporin A-induced toxicity without affecting its therapeutic activity. Many protective agents have shown promising results, such as N-acetylcysteine, curcumin, coenzyme Q10, etc. (Ahmed et al., 2013; Sagiroglu et al., 2014; Abdelkader et al., 2021). Another recorded neuroprotective agent is Cerebrolysin, which was tested in the present study.

In the current study, in the combined group IV (Cyclosporin A + Cerebrolysin group), animals received a daily intraperitoneal injection (I.P.) of 2.5 ml/kg of Cerebrolysin for 4 weeks concomitant with daily cyclosporine administration at a dose of 25 mg/kg/day dissolved in olive oil, orally by gavage for 4 weeks. Results of the present study revealed that Cerebrolysin could prevent almost all histopathological alterations in the cerebellar cortex induced by cyclosporin A. Examination of H and E-stained sections revealed Purkinje cells that were nearly as the control group. Cresyl-fast violet-stained sections showed an increase in purple Nissl's granules in the perikaryal of Purkinje cells compared to those of group III. This was in accordance with Sharma et al. (2023), who examined Nissl-stained nerve cells in spinal cord dorsal and ventral horns and found that treatment with Cerebrolysin markedly attenuated nerve cell injury after induced nerve lesion with Cu or Ag nanoparticle intoxication.

The results of the TEM examination of cerebrolysin-treated animals confirmed those of the light microscope. The Purkinje cell, with its main dendrite and large oval euchromatic nucleus, was nearly similar to that of the control group. Numerous mitochondria, well-developed rough endoplasmic reticulum cisternae, and lysosomes were visible in the cytoplasm. Granule cells were nearly similar to the control group, with rounded or oval nuclei and clumps of heterochromatin. A rim of cytoplasm around the granule cell nucleus showed free ribosomes and mitochondria. Astrocytes with electron-dense cytoplasm and well-myelinated nerve fibers were also shown.

The presence of astrocytes was noticed in the electron microscopic examination of the cerebrolysin group. This was confirmed immunohistochemically by examination of sections stained with glial fibrillary acidic protein (GFAP) from such a group in which positive GFAP expression was more or less comparable to that seen in control rat research. Our results were in agreement with Abdel-Aziz et al. (2019) who evaluated the effectiveness of Cerebrolysin on adult male albino rats' dendate gyrus of the hippocampus following experimentally generated acute ischemic stroke and found a positive cytoplasmic reaction in astrocytes. Moreover, co-treatment with Cerebrolysin significantly improved the gait performance of animals by increasing the stride width of their footprint patterns.

All the improved findings could be attributed to the Cerebrolysin. Its neurotrophic benefits are mediated by its capacity to reduce inflammation, free radical production, and excitotoxicity (Nasrolahi et al., 2018; Moghazy et al., 2019; El-Marasy et al., 2021). Tharwat et al. (2023) added that Cerebrolysin could reduce the rise in peroxidation of lipids brought on by reserpine in the striatum and raise the levels of striatal and midbrain malondialdehyde (MDA) and glutathione (GSH), indicating Cerebrolysin potential therapeutic effect in reserpine-induced Parkinson's disease (PD) in an animal model.

Moreover, Sharma et al. (2023) found that Cerebrolysin therapy dramatically decreased the buildup of inflammatory cytokines and significantly enhanced anti-inflammatory cytokines in the spinal cord after the 10th week of a nerve lesion, either with or without nanoparticle exposure. Accordingly, they concluded that Cerebrolysin could reduce neuropathic pain flare-ups, blood-spinal-cord barrier permeability, and cord pathology following chronic intoxication with nanoparticles.

Additionally, in the current study, the presence of well-myelinated nerve fibers in the combined group can be attributed to the capacity of Cerebrolysin for the regeneration of neurons. Its structure, which includes low-molecular-weight peptides and amino acids with neuroprotective qualities like glial cell-derived neurotrophic factor and insulin-like growth factors 1 and 2, was primarily responsible for this (Kim et al., 2019).

However, few distorted and shrunken Purkinje cells and wide intercellular spaces were still shown in H&E-stained sections of rats' cerebella of group IV (Cyclosporin A + Cerebrolysin group). Additionally, TEM examination of such a group revealed a slightly irregular nucleus of one Purkinje cell, vacuolations in the axoplasm of a few nerve fibers, and a few empty spaces between the cells in the neuropil. This can be explained by Abolhasanpour et al. (2019) who suggested that the result of Cerebrolysin in their study was dose- and time-dependent. They found that Cerebrolysin injection at a dose of 1 mL/kg for 1 week showed a slight improvement in overactive neurogenic detrusors in female rats with spinal cord injuries. Nevertheless, bladder compliance was enhanced by 2.5 mL/kg of Cerebrolysin infusion for 4 weeks in spite of some weak contractions.

Additionally, the bladder pressure pattern in the rats administered 2.5 mL/kg exhibited a pattern that was comparable to the normal control group. Sharma et al. (2023) provided confirmation of this when they concluded that the higher doses of Cerebrolysin had similar neuroprotective effects in rats with nerve lesions and nanoparticle intoxication.

Conclusion

According to the results of the present research, Cerebrolysin has an ameliorative effect against cyclosporin A-induced cerebellar toxicity in adult male albino rats.

Recommendation

The authors recommend further clinical trials to confirm the ameliorative effect of Cerebrolysin against cyclosporin A-induced cerebellar toxicity in order to use Cerebrolysin prior to and during the treatment of cyclosporin A to avoid such toxicity.

Acknowledgement

Conflict of Interest

No conflicts of interest were reported by the authors.

References

Abdelkader, M., Hilal, M., Torky, A.R., et al. (2021) 'Experimental study of renal toxicity of cyclosporine and the ameliorative effect of N-acetylecysteine in albino rat', *Ain Shams Journal of Forensic Medicine and Clinical Toxicology*, 37(2), pp. 8–15. Available at: https://doi.org/10.21608/ajfm.2021.17 4400.

Abolhasanpour, N., Eidi, A., Hajebrahimi, S., et al. (2019) 'Effect of cerebrolysin on bladder function after spinal cord

injury in female Wistar rats', *International Journal of Urology: Official Journal of the Japanese Urological Association*, 26(9), pp. 917–923. Available at:

https://doi.org/10.1111/iju.14059.

Ahmed, G., Siam, M.G., Shaban, S. and Awwad, I. (2013) 'The role of coenzyme Q10 against cyclosporine-A induced cardiotoxicity in adult male albino rats (histological and toxicological study)', *Ain Shams Journal of Forensic Medicine and Clinical Toxicology*, 20(1), pp. 18–29. Available at:

https://doi.org/10.21608/ajfm.2013.19 383.

Cattoretti, G., Pileri, S., Parravicini, C., et al. (1993) 'Antigen unmasking on formalin-fixed, paraffin-embedded tissue sections', *The Journal of Pathology*, 171(2), pp. 83–98. Available at:

https://doi.org/10.1002/path.17117102 05.

DeAngelo, V., Gehan, A., Paliwal, S., et al. (2023) 'Cerebellar activity in hemi-parkinsonian rats during volitional gait and freezing'. *bioRxiv*, p. 2023.02.28.530475. Available at:

https://doi.org/10.1101/2023.02.28.53 0475.

El-azab, N., Elmahalaway, A. and Sabry, D. (2018) 'Effect of methyl mercury on the cerebellar cortex of rats and the possible neuroprotective role of mesenchymal stem cells conditioned medium. histological and immunohistochemical study', *Journal of Gastrointestinal Cancer and Stromal Tumors*, 08. Available at:
https://doi.org/10.4172/2572-4126.1000430.

El-Marasy, S.A., El Awdan, S.A., Hassan, A., et al. (2021) 'Anti-depressant effect of cerebrolysin in reserpine-induced depression in rats: Behavioral, biochemical, molecular and immunohistochemical evidence', *Chemico-Biological Interactions*, 334, p. 109329. Available at:

https://doi.org/10.1016/j.cbi.2020.109 329.

Faheem, S., Moustafa, Y., El- Sayed, N., et al. (2022) 'Mechanisms of cyclosporin A induced hepatotoxicity', *Records of Pharmaceutical and Biomedical Sciences*, 6(1), pp. 57–68. Available at:
https://doi.org/10.21608/rpbs.2022.12 9863.1133.

Feagan, B.G., McDonald, J., Rochon, J., et al. (1994) 'Low-dose cyclosporine for the treatment of Crohn's Disease', *New England Journal of Medicine*, 330(26), pp. 1846–1851. Available at: https://doi.org/10.1056/NEJM1994063 03302602.

Flores, C., Fouquet, G., Moura, I.C., et al. (2019) 'Lessons to learn from low-dose cyclosporin-A: A new approach for unexpected clinical applications', *Frontiers in Immunology*, 10. Available at:

https://doi.org/10.3389/fimmu.2019.0 0588.

Fonnum, F. and Lock, E.A. (2000) 'Cerebellum as a target for toxic substances', *Toxicology Letters*, 112–113, pp. 9–16. Available at: https://doi.org/10.1016/s0378-4274(99)00246-5.

Gaalen, V.J., Kerstens, F.G., Maas, R.P., et al. (2014) 'Drug-induced cerebellar ataxia: A systematic review', *CNS Drugs*, 28(12), pp. 1139–1153. Available at:

https://doi.org/10.1007/s40263-014-0200-4.

Hasan, W., Kori, R.K., Jain, J., et al. (2020) 'Neuroprotective effects of mitochondria-targeted curcumin against rotenone-induced oxidative damage in cerebellum of mice', *Journal of Biochemical and Molecular Toxicology*, 34(1), p. e22416. Available at:

https://doi.org/10.1002/jbt.22416.

Hayat, M.A. (2000) *Principles and Techniques of Electron Microscopy: Biological Applications*. Cambridge University Press. Available at: https://books.google.com.bh/books?id=nfsVMH8it1kC.

Jorgačevski, J. and Potokar, M. (2023) 'Immune functions of astrocytes in viral neuroinfections', *International Journal of Molecular Sciences*, 24(4), p. 3514. Available at:

https://doi.org/10.3390/ijms24043514.

Kara, H., Çağlar, C., Asiltürk, M., et al. (2021) 'Comparison of a manual walking platform and the CatWalk gait analysis system in a rat osteoarthritis model', *Advances in Clinical and Experimental Medicine: Official Organ Wroclaw Medical University*, 30(9), pp. 949–956. Available at:

https://doi.org/10.17219/acem/137536.

Khalaf, A.A.; Zaki, A.R.; Galal, M.K., et al. (2017) 'The potential protective effect of α-lipoic acid against nanocopper particle-induced hepatotoxicity in male rats''. *Hum. Exp. Toxicol.* 36, 881–891.

Kim, J.Y., Kim, H.J., Choi, H.S., et al. (2019) 'Effects of cerebrolysin A in patients with minimally conscious state after stroke: An observational retrospective clinical study', *Frontiers in Neurology*, 10, p. 803. Available at: https://doi.org/10.3389/fneur.2019.00803.

Layton, C. and Suvarna, K. (2013) *Bancroft's Theory and Practise of Histological Techniques (7th edition) (Co-author)*.

Liddicoat, A.M. and Lavelle, E.C. (2019) 'Modulation of innate immunity by cyclosporine A', *Biochemical Pharmacology*, 163, pp. 472–480. Available at:

https://doi.org/10.1016/j.bcp.2019.03.022.

Lu, Y., Li, C.F., Ping, N.-N., et al. (2020) 'Hydrogen-rich water alleviates cyclosporine A-induced nephrotoxicity via the Keap1/Nrf2 signaling pathway', *Journal of Biochemical and Molecular Toxicology*, 34(5), p. e22467. Available at:

https://doi.org/10.1002/jbt.22467.

Mahmoudi, S., Farshid, A.A., Tamaddonfard, E., et al. (2022) 'Behavioral, histopathological, and biochemical evaluations on the effects of cinnamaldehyde, naloxone, and their combination in morphine-induced cerebellar toxicity', *Drug and Chemical Toxicology*, 45(1), pp. 250–261. Available at:

https://doi.org/10.1080/01480545.2019.1681446.

Makary, E.F.Y., Ali, E.A.I., Fargali, L.M. et al. (2015) 'Gingko Biloba versus neuropeptide derivative FPF 1070 (Cerebrolysin) effect against cisplatin-induced sciatic neuropathy.' *Austin Journal of Neurosurgery*. 2(3): ID1036. ISSN : 2381-8972

Masliah, E. and Díez-Tejedor, E. (2012) 'The pharmacology of neurotrophic treatment with Cerebrolysin: brain

protection and repair to counteract pathologies of acute and chronic neurological disorders', *Drugs of today (Barcelona, Spain*, 48 Suppl A, pp. 3–24. Available at: https://doi.org/10.1358/dot.2012.48(su ppl.a).1739716.

Mescher, A.L. (2016) *Junqueira's Basic Histology Text & Atlas (14th ed.). E-book Research Gate.* Available at: https://www.researchgate.net/publicati on/283490690_Junqueira's_Basic_His tology_Text_Atlas_14th_ed (Accessed: 11 June 2023).

Moghazy, A.M., Saad, A.A. and haridy, S.A. (2019) 'The potential antidepressant effect of adenosine triphosphate and cerebrolysin on reserpine induced depression in male rats.', *International Journal of Advanced Research*, 7, pp. 540–553. Available at: https://doi.org/10.21474/IJAR01/8360.

Mohamed, H.K. and Mohamed, H.Z.-E.-A. (2018) 'A histological and immuno-histochemical study on the possible protective role of silymarin on cerebellar cortex neurotoxicity of lactating albino rats and their pups induced by gibberellic acid during late pregnancy and early postnatal period', *Egyptian Journal of Histology*, 41(3), pp. 345–371. Available at: https://doi.org/10.21608/ejh.2018.301 9.1001.

Nagib M.M., Tadros M.G., Abd Al-khalek H.A., et al. (2018) 'Molecular mechanisms of neuroprotective effect of adjuvant therapy with phenytoin in pentylenetetrazole-induced seizures: Impact on Sirt1/NRF2 signaling pathways'. *Neurotoxicology.* 2018;68: 47–65. doi: 10.1016/j.neuro.2018.07.006.

Nasrolahi, A., Mahmoudi, J., Akbarzadeh, A., et al. (2018) 'Neurotrophic factors hold promise for the future of Parkinson's disease treatment: Is there a light at the end of the tunnel?' *Reviews in the Neurosciences*, 29(5), pp. 475–489. Available at: https://doi.org/10.1515/revneuro-2017-0040.

Ovalle, W.K., Nahirney, P.C. (2020) *Netter's Essential Histology. E-book library* [online]. Available at: https://books.google.com/books/about/ Netter's_Essential_Histology_E_Book .html?hl=ar&id=StnNDwAAQBAJ (Accessed: 11 June 2023).

Pharmacoeconomic Review Report: Ixekizumab (Taltz): (Eli Lilly Canada Inc.): Indication: Treatment of adult patients with active psoriatic arthritis who have responded inadequately to, or are intolerant to one or more disease-modifying antirheumatic drugs (DMARD). Taltz can be used alone or in combination with a conventional DMARD (e.g., methotrexate) (2018). Ottawa (ON): Canadian Agency for Drugs and Technologies in Health (CADTH Common Drug Reviews). Available at: http://www.ncbi.nlm.nih.gov/books/N BK539537/ (Accessed: 11 June 2023).

Ponticelli, C. and Glassock, R.J. (2019) 'Prevention of complications from use of conventional immunosuppressants: a critical review', *Journal of Nephrology*, 32(6), pp. 851–870. Available at: https://doi.org/10.1007/s40620-019-00602-5.

Pradier, A., Papaserafeim, M., Li, N., et al. (2019) 'Small-molecule immuno-suppressive drugs and therapeutic

immunoglobulins differentially inhibit NK cell effector functions in vitro', *Frontiers in Immunology*, 10, p. 556. Available at: https://doi.org/10.3389/fimmu.2019.00556.

Rafati, A., Erfanizadeh, M., Noorafshan, A., et al. (2015) 'Effect of benzene on the cerebellar structure and behavioral characteristics in rats', *Asian Pacific Journal of Tropical Biomedicine*, 5(7), pp. 568–573. Available at: https://doi.org/10.1016/j.apjtb.2015.05.002.

Roshan, K.S., Spano, A.D., McKinney, A.M., et al. (2017) 'Potentially reversible acute cerebellar toxicity associated with Minnelide', *Neuroradiology*, 59(4), pp. 419–421. Available at: https://doi.org/10.1007/s00234-017-1809-z.

Ruozi, B., Belletti, D., Sharma, H.S., et al. (2015) 'PLGA nanoparticles loaded cerebrolysin: studies on their preparation and investigation of the effect of storage and serum stability with reference to traumatic brain injury', *Molecular Neurobiology*, 52(2), pp. 899–912. Available at: https://doi.org/10.1007/s12035-015-9235-x.

Sagiroglu, T., Kanter, M., Yagci, M.A., et al. (2014) 'Protective effect of curcumin on cyclosporin A-induced endothelial dysfunction, antioxidant capacity, and oxidative damage', *Toxicology and Industrial Health*, 30(4), pp. 316–327. Available at: https://doi.org/10.1177/0748233712456065.

Shah, S.Z.A., Hussain, T., Zhao, D., et al. (2017) 'A central role for calcineurin in protein misfolding neuro-degenerative diseases', *Cellular and Molecular Life Sciences*, 74(6), pp. 1061–1074. Available at: https://doi.org/10.1007/s00018-016-2379-7.

Shalabi, N. and Sarhan, N. (2008) 'Light and electron microscopic study on the effect of valproic acid on cerebellar cortex of adult male albino rats and the possible protective effect of l-carnitine', *Egyptian Journal of Histology*, 31, pp. 256–265.

Sharma, H.S., Feng, L., Chen, L., et al. (2023) 'Cerebrolysin attenuates exacerbation of neuropathic pain, blood-spinal cord barrier breakdown and cord pathology following chronic intoxication of engineered Ag, Cu or Al (50-60 nm) nanoparticles', *Neurochemical Research* [Preprint]. Available at: https://doi.org/10.1007/s11064-023-03861-8.

Sherif, R. (2017) 'Effect of cerebrolysin on the cerebellum of diabetic rats: An imunohistochemical study.' Journal of Tissue and Cell;49 (6): 726-733

Sovcikova, A.; Tulinska, J.; Kubova, J. et al. (2002) 'Effect of cyclosporin A in Lewis rats in vivo and HeLa cells in vitro.' Journal of Applied Toxicology; 22(3):153- 160.

Sun, S.-L., Liu, J.-J., Zhong, B., et al. (2019) 'Topical calcineurin inhibitors in the treatment of oral lichen planus: a systematic review and meta-analysis', *The British Journal of Dermatology*, 181(6), pp. 1166–1176. Available at: https://doi.org/10.1111/bjd.17898.

Tapia, C., Nessel, T.A. and Zito, P.M. (2022) 'Cyclosporine', in *StatPearls*. Treasure Island (FL): StatPearls

Publishing. Available at: http://www.ncbi.nlm.nih.gov/books/NBK482450/ (Accessed: 6 March 2023).

Teimouri, A., Ahmadi, S.R., Ardakani, S.A., et al. (2022) 'Cyclosporine-A-based immunosuppressive therapy-induced neurotoxicity: A case report', *Open Access Emergency Medicine* [Preprint]. Available at: https://www.tandfonline.com/doi/abs/10.2147/OAEM.S241501 (Accessed: 6 March 2023).

Tharwat, E.K., Abdelaty, A.O., Abdelrahman, A.I., et al. (2023) 'Evaluation of the therapeutic potential of cerebrolysin and/or lithium in the male Wistar rat model of Parkinson's disease induced by reserpine', *Metabolic Brain Disease*, 38(5), pp. 1513–1529. Available at: https://doi.org/10.1007/s11011-023-01189-4.

Vangaveti, S.; Das, P.; Kumar, V.L. et al. (2021) ''Metformin and silymarin afford protection in cyclosporine A induced hepatorenal toxicity in rat by modulating redox status and inflammation''. *J. Biochem. Mol. Toxicol.* 35, e22614.

Weil, M.-T., Möbius, W., Winkler, A., et al. (2016) 'Loss of myelin basic protein function triggers myelin breakdown in models of demyelinating diseases', *Cell Reports*, 16(2), pp. 314–322. Available at:

https://doi.org/10.1016/j.celrep.2016.06.008.

Wright, M., Skaggs, W. and Nielsen, F.A. (2016) 'The cerebellum', *WikiJournal of Medicine*, [Preprint]. Available at: https://search.informit.org/doi/abs/10.3316/informit.380776158668038 (Accessed: 6 March 2023).

Xin, G.L.L., Khee, Y.P., Ying, T.Y., et al. (2019) 'Current status on immunological therapies for type 1 diabetes mellitus', *Current Diabetes Reports*, 19(5), p. 22. Available at: https://doi.org/10.1007/s11892-019-1144-3.

Yang, Z. and Wang, K.K.W. (2015) 'Glial fibrillary acidic protein: from intermediate filament assembly and gliosis to neurobiomarker', *Trends in Neurosciences*, 38(6), pp. 364–374. Available at:

https://doi.org/10.1016/j.tins.2015.04.003.

Zhang, L., Chopp, M., Meier, D.H., et al (2013) 'Sonic hedgehog signaling pathway mediates cerebrolysin-improved neurological function after stroke', *Stroke*, 44(7), pp. 1965–1972. Available at:

https://doi.org/10.1161/STROKEAHA.111.000831.

Zurita, E., Huerta, M., De Jesús, L., et al. (2017) 'Cerebrolysin effects on cardiac neuropathy in diabetic rats', *Pharmacology & Amp; Pharmacy*, 08(07), pp. 215–230. Available at: https://doi.org/10.4236/pp.2017.8701.

التأثير العلاجي المحتمل للسيريبروليسين ضد السمية المخيخية المستحثة بالسيكلوسبورين أ ـ في ذكور الجرذان البيضاء البالغة

حورية عرفات¹ ، جورج ناجى رفعت² ، منى محمد عونى³ ، إيرينى فكرى¹

١ قسم الهستولوجيا وبيولوجيا الخلية ـ كلية الطب ـ جامعة قناة السويس
٢ أقسام الباطنة والقلب ـ هيئة قناة السويس
٣ قسم الطب الشرعى و السموم ـ كلية الطب ـ جامعة قناة السويس

السيكلوسبورين أ هو عامل مثبط للمناعة يستخدم لعلاج رفض العضو بعد الزرع وأمراض المناعة الذاتية. يمكن أن تحدث تأثيرات سامة على القشرة المخيخية مثل ترنح المخيخ ، وذمة وعائية المنشأ والآفات فوق المحصنة العرضية. يمتلك السيريبروليسين استراتيجيات علاجية كعامل تغذوي عصبي مع تأثيرات حماية للاعصاب. و قد هدف هذا العمل إلى تقييم التأثير العلاجي المحتمل للسيريبروليسين على السمية المخيخية التي يسببها السيكلوسبورين أ في ذكور الجرذان البيضاء البالغة. تم اختيار ٤٠ جردًا بالغًا من ذكور الجرذان البيضاء بشكل عشوائي إلى ٤ مجموعات وتلقوا جميع العلاجات لمدة ٤ أسابيع. المجموعة الأولى ، بمثابة المجموعة الضابطة. المجموعة الثانية ، تم إعطاء السيريبروليسين حقنة يومية داخل الصفاق ٢,٥ مل / كجم. تلقت المجموعة الثالثة السيكلوسبورين أ يوميًا بجرعة ٢٥ مجم / كجم / يوم مذاب في زيت الزيتون عن طريق الفم. تم إعطاء المجموعة الرابعة ، السيكلوسبورين أ المصاحب للسيريبروليسين. بعد ٤ أسابيع ، تم ذبح الفئران عن طريق قطع الرأس. تم إستخدام الهيماتوكسيلين والأيوسين، و الكريسيل البنفسجي السريع، والصبغة الهستوكيميائية المناعية للبروتين الليفي الدبقي، والفحص المجهري الإلكتروني وتقييم المشية. فى المجموعة الثالثة والتى تلقت السيكلوسبورين أ ظهرت خلايا البركنجي والخلايا الحبيبية غير منتظمة مع نوى غير منتظمة. تحتوي الألياف العصبية على غمد المايلين الخافت و / أو مناطق بؤرية من تشققات المايلين. و كانت الخلايا الإيجابية للبروتين الليفي الدبقي الحمضي أقل وفرة مع قلة حبيبات نيسل وضعف المشية. أعاد السيريبروليسين معظم التغيرات النسيجية المرضية والسلوك الحركي. السيريبروليسين له تأثير مخفف على السمية المخيخية التي يسببها السيكلوسبورين أ في ذكور الجرذان البيضاء البالغة.